Experimentally-based in-plane drift limits for the upper threshold of masonry light damage

Korswagen, Paul A.; Rots, Jan G.; Terwel, Karel C.

DOI
10.1002/eqe.4246

Publication date
2024

Document Version
Final published version

Published in
Earthquake Engineering and Structural Dynamics

Received: 21 June 2024 | Revised: 20 September 2024 | Accepted: 22 September 2024

DOI: 10.1002/eqe.4246

RESEARCH ARTICLE

WILEY

Experimentally-based in-plane drift limits for the upper threshold of masonry light damage

Paul A. Korswagen | **Jan G. Rots** | **Karel C. Terwel**

Faculty of Civil Engineering and Geosciences, Delft University of Technology, Delft, The Netherlands

Correspondence
Paul A. Korswagen, Faculty of Civil Engineering and Geosciences, Delft University of Technology, Delft, The Netherlands.
Email: P.A.KorswagenEguren@tudelft.nl

Funding information
Nederlandse Aardolie Maatschappij; Instituut Mijnbouwschade Groningen

Abstract

Drift limits are useful thresholds; during design or retrofitting analyses, engineers can compare the expected behaviour of a structure to drift limits that predict when the structure will reach a certain condition. This helps ensure that structures satisfy specified performance goals when exposed to certain hazards. Masonry walls are susceptible to damage from lateral in-plane actions such as wind or earthquake loading; ensuring that in-plane drift remains sufficiently small will help limit this damage. Drift limits based on crack-based damage are scarce, however, with DS1 limits being extrapolated from higher damage grades based on structural strength capacity or ductility. In this work, crack-based damage is evaluated on a multitude of full-scale experimental walls surveyed with digital image correlation. This method observes the initiation and propagation of cracking. Cyclically incremental in-plane tests provide a range of drift-damage relationships. These are explored with machine learning to determine influential predictors and ultimately establish drift limits for light damage. Two types of brick masonry are explored: fired-clay and calcium-silicate. For the latter, light damage begins at an in-plane drift of 0.5 mm/m and can extend to 4.8 mm/m (or 0.48%) for the former before the masonry surpasses light damage and reaches structural damage grades. In comparison to drift limits set by other authors and (international) guidelines to characterise light damage, significant damage, or the ultimate capacity of masonry walls, the resulting drift limits for light damage from this work are set directly on the basis of experiments and are in good agreement with other authors. Most importantly, all the consulted values for ultimate capacity are much larger than the upper threshold for light damage determined herein, with limits for significant damage in the same order of magnitude. This result verifies the accuracy of the experimental crack-based characterisation used to establish the drift thresholds.

KEYWORDS
calcium-silicate brick, clay brick, cracks, drift, light damage, masonry

1 | INTRODUCTION

In the realm of structural engineering, the determination of drift limits stands as a pivotal aspect in assessing the performance and resilience of buildings subjected to lateral forces such as wind or those induced by vibrations.[1,2] Drift limits serve as invaluable thresholds, facilitating a comprehensive understanding of a structure's behaviour under dynamic loading conditions[3] and some quasi-static actions like differential settlements.[4] Engineers, during the design or retrofitting phases, routinely employ drift limits as robust metrics to gauge and ensure the structural integrity of a building, with the aim of meeting specified performance goals when exposed to various hazards.[5]

Masonry walls, a fundamental component of many structures, especially in housing applications in the Netherlands, are particularly susceptible to damage resulting from in-plane actions.[6] It is imperative to verify that in-plane drift remains within acceptable limits to mitigate the risk of (structural) damage.[7–9] Within performance-based design, frequent vibrations or wind loads should be considered such that masonry components do not enter light damage. Drift limits provide a useful tool for this analysis.[10]

The current landscape of drift limits for masonry walls often encounters limitations, especially when not derived from crack-based damage assessments. Notably, existing limits, especially those used for DS1 (damage state one as proposed by the EMS[11]), are frequently extrapolated from higher damage grades predicated on structural strength capacity or ductility.[1,12,13] This extrapolation poses challenges in accurately predicting the threshold at which damage becomes a concern, highlighting the need for more nuanced and experimentally-derived drift limits. These offer a more granular and realistic understanding of a masonry wall's response to lateral forces. Unlike model-based or extrapolation-based limits, experimentally-derived thresholds provide a direct and precise measure of the drift at which damage initiates.[14–16] A clear definition of damage must be applied, however.

Most experiments on in-plane walls have focused on establishing thresholds at which the strength capacities of the components are compromised: these represent the ultimate limit state or near-collapse.[3,17] Limits, at which damage begins, where mechanical damage is related to crack-based damage in masonry, have seldom been quantified or have been extrapolated from the shape of force-displacement curves.[18,19] Crack-based light damage, ranging from just-visible cracks to wider cracks not yet compromising the capacity of a wall or component, is nevertheless important to quantify repair and maintenance costs, to prevent additional damage (such as the ingress of water into the structure), or to distinguish the attributability of the damage from various actions.

To define experimental drift limits suitable for light damage, masonry walls have been tested at small, repeated, cyclic values of drift throughout several campaigns at the Delft University of Technology while monitoring crack initiation and propagation.[20–22] The outcome of these tests is analysed in the present work in terms of the relationship between drift and damage with the goal of determining when light damage begins and when it can be considered to end. The paper starts with a brief overview of the tests performed and continues with an investigation of drift and crack-based damage from the experiments as measured with the Ψ parameter which quantifies damage using the width (w), the number (n), and the length (L) of cracks as per Equation (1).[23] At a value of Ψ equal to 1, cracks in the order of 0.1 mm in width start to become visible. A discussion including a comparison to other drift limits and a wrap-up conclusion, are presented at the end of the paper.

$$\Psi = 2 \cdot n^{0.15} \cdot c_w^{0.3} \quad c_w = \frac{\sum_{i=1}^{n} w_i^2 \cdot L_i}{\sum_{i=1}^{n} w_i \cdot L_i} \quad (1)\ \text{Definition of } \Psi$$

This scheme is shown in Figure 1 where the methodology of the paper is described in a flow chart. The experimental tests and the definition of light damage from earlier work are brought up to post-process digital-image-correlation measurements from the tests to determine cracking behaviour. This becomes the response variable in a machine learning classification problem that includes other features from the test such as the wall geometries and setup boundaries, though ultimately isolating drift as the main predictor for damage. Moreover, drift thresholds are defined for two types of masonry, namely fired-clay and calcium-silicate brick masonry.

2 | SUMMARY OF EXPERIMENTAL TESTS ON MASONRY WALLS

To characterise the cracking behaviour of masonry at the component scale, that is, to observe how cracks initiate and propagate on full-size elements such as walls, several types of experiments have been conducted. In parallel, tests focused on

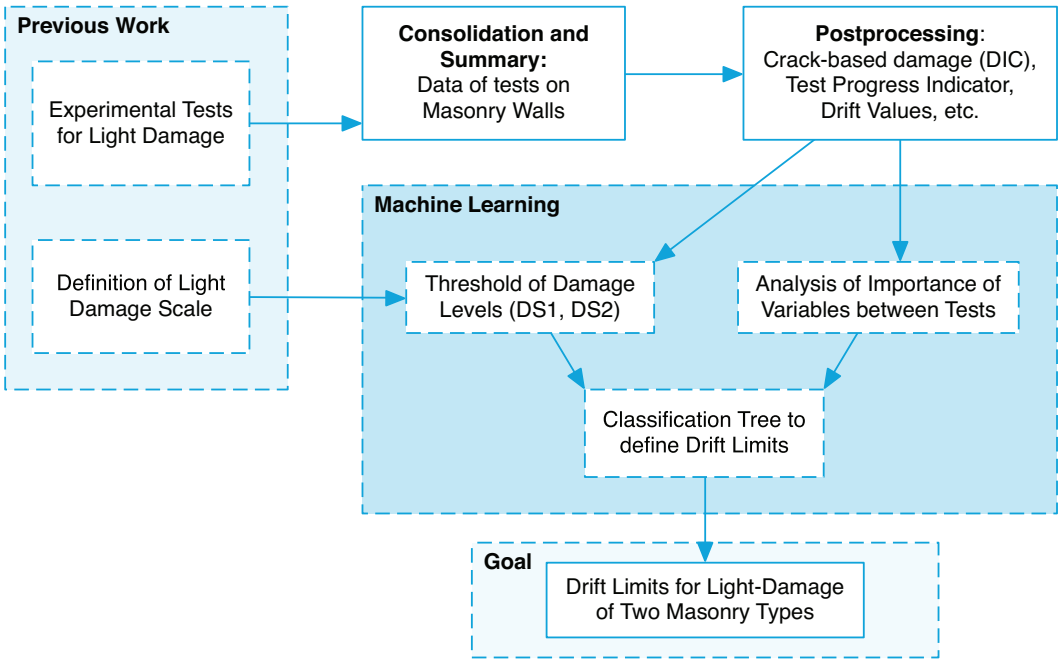

FIGURE 1 Flowchart of this paper with the goal of obtaining drift limits for the light damage of masonry walls.

the fracture mechanics of masonry, at the brick-to-brick scale in tension and shear were analysed, while smaller wallettes were included to investigate compressive properties and predominantly vertical cracking in in-plane flexure. The focus, however, was placed on walls about 3.1 meters wide and 2.7 meters tall built of single wythe (about 100 mm) brick masonry in a stretcher bond pattern. Over several campaigns, twenty walls have been tested with a light damage protocol[20,21] and sixteen of them were driven to near-collapse. The various campaigns focused on different brick materials, initial conditions such as existing cracks represented by 'unbonded' joints, varying cycle repetitions, openings, differing boundary conditions, etc. A common thread throughout these campaigns, however, was the light damage protocol consisting of a large number of repeated, incremental cycles surveyed by digital image correlation (DIC).[24,16] In this context, it is possible to link the applied in-plane drift to the cracked conditions of the masonry.

Figure 2 and Table 1 present an overview of the twenty walls. Three fired-clay and three calcium-silicate brick masonry geometries are distinguished; these wall types are listed from A to F. Furthermore, the boundary condition applied to the walls is described as either 'cantilever', where the top support was displaced horizontally but allowed to rotate, or 'fixed' a.k.a as 'double-clamped', where the top support was displaced horizontally but kept parallel to the bottom support. The loading protocol has three or two stages. First, a one-way, cyclic in-plane drift is enforced with five or six steps of repeated cycles. The amplitude of the first step is that which causes a value of $\Psi = 1$; this is repeated 3, 10, 20 or 30 times before increasing this amplitude by 25% for the following step. The magnitude of the increase is kept constant. Second, a two-way cyclic (with both positive and negative) drift is applied. The magnitude of the steps is the same as for the one-way cycles with up to seven steps, meaning that the amplitude of the last step is 2.75 times larger than the first step. Each step consists of 30 or 50 cycles. Third, a near-collapse protocol is applied which comprises fixed displacements: 10×2.3 mm, 2×2.7 mm, 2×8.1 mm, 1×13 mm, 1×27 mm, 1×40 mm, 1×54 mm, 1×67 mm and 1×81 mm though the tests might be terminated before the last step. Alternative to the repetitive and cyclic protocols, an asymmetric light-damage protocol may be employed. This one includes cycles in both directions, but the amplitude of the cycles in one direction is halved. For additional details on the loading protocols, the reader is referred to.[14,15,3]

Figure 3 provides a comparison between the different stages of the test for one of the walls. It can be observed how the repetitive stage only includes drift values in one direction and is associated with a reduction or degradation of the force of each repetition of the drift; the force remains mostly positive. Some residual drift is accumulated towards the end of his stage. The cyclic phase includes drifts in the opposite direction. One can observe how most of the force degradation in the positive direction has already occurred while the negative drift still leads to a reduction of the force within every step. This force degradation is linked to a propagation of the cracks in both width and length. Finally, the near collapse stage offers a more familiar picture with large reductions in lateral capacity at increased drift and a considerable hysteresis envelope during shear failure.

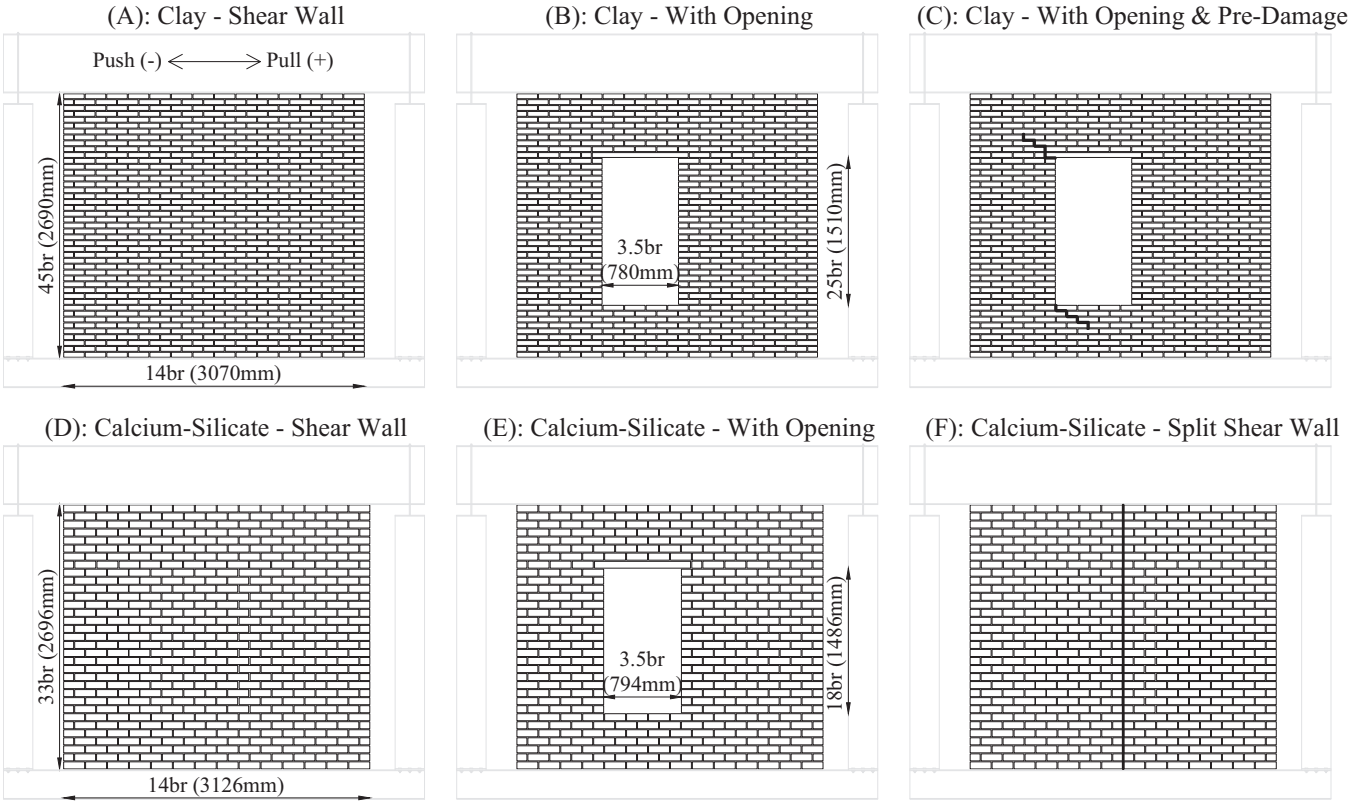

FIGURE 2 Scheme of various wall types tested during the light-damage campaign to characterise crack propagation in solid fired-clay (CLBR) and calcium-silicate brick (CSBR) masonry walls.

The repetitive, cyclic, and asymmetric protocols enforce in-plane drift values that reach up to the maximum force capacity of the specimens. Up until this point cracking develops and later worsens during the near-collapse stage until the final failure mechanism. Through the experiments, DIC is used to measure a displacement field of the entire surface of the walls on a grid of 2.7 × 2.7 mm with a precision of 25 μm. This means that cracks anywhere on the walls can be tracked accurately. Figure 4 shows examples of different cracking patterns for some of the walls. Note that the crack characterisation is done retroactively, meaning that cracks which later fuse together are also considered one crack at the beginning of the analyses, such as the case of specimen of type A, Comp47. In this manner, the width, length and number of cracks on each wall is tracked automatically throughout the entire tests. On most walls, cracks progressed horizontally or diagonally, usually propagating off the corners of openings or the sides of the walls. For every value of drift and at the intermediate zero drift value, a record of the cracks was captured and the value of Ψ automatically computed.

3 | RESULTS: RELATIONSHIP BETWEEN CRACK-BASED DAMAGE AND IN-PLANE DRIFT

The intensity of damage is characterised by the cracks on the walls using Ψ. These are plotted in Figure 5 against the absolute value of drift. However, Figure 5 includes two horizontal and four vertical thresholds which are dissected in this section. The former correspond to the values of Ψ that establish the transition into and out of light damage. The latter are the drift values that are the goal of this paper. Note that drift is plotted on a logarithmic scale which suggests an exponential relationship to damage.

3.1 | Thresholds for light damage

The lowest values of Ψ that can be accurately measured by the DIC system are around 1 with at least one crack with a maximum width of 0.1 mm and a minimum length of 100 mm, or two cracks of slightly narrower width (70 μm). Since the

TABLE 1 Overview of full-scale walls tested and their corresponding (cyclic) protocols. See Figure 2 for wall types. Boundaries are cantilever or fixed.

Wall name	Wall type	Lab boundary	Year built	Protocol		
				Repetitive	Cyclic	Near collapse
Comp40	B	C	2017	5 × 3	7 × 50	81 mm
Comp41	B	C	2017	5 × 10	7 × 30	40 mm
Comp42	B	C	2017	6 × 20	7 × 30	40 mm
Comp43	B	C	2017	NA	7 × 50	40 mm
Comp44	B	C	2017	6 × 20	NA	NA
Comp45	C	C	2018	5 × 30	7 × 30	NA
Comp46	C	C	2018	5 × 30	7 × 30	81 mm
Comp47	A	F	2018	A 7 × 10		27 mm
Comp48	A	F	2018	A 7 × 10		NA
Comp49	E	C	2018	5 × 30	7 × 30	40 mm
Comp50	E	C	2018	5 × 30	7 × 30	40 mm
Comp51	E	C	2021	5 × 30	7 × 30	81 mm
Comp52	E	C	2021	5 × 30	7 × 30	81 mm
Comp53	E	F	2021	5 × 30	7 × 30	40 mm
Comp54	B	C	2021	5 × 30	5 × 30	NA
Comp55	B	F	2021	6 × 30	8 × 30	27 mm
Comp56	B	F	2021	5 × 30	7 × 30	27 mm
Comp57	D	F	2021	A 7 × 10		40 mm
Comp58	F	F	2021	A 7 × 10		67 mm
Comp59	F	F	2021	A 7 × 10		54 mm

narrower end of a crack must also be reliability detected, in practice, the lowest values of Ψ measured are slightly above 1. This means that the threshold for the beginning of light damage must be a bit larger. This value and the one for the end of light damage are determined by 'kmeans' clustering to help establish optimum categories.[25] Additionally, these are verified iteratively by maximising the true positive rate and minimising the false positive rate of a classification model[26] while maintaining some realistic values.

The upper threshold of $\Psi = 4$, which corresponds to two or three cracks of 5 to 6 mm in width, follows from clustering the data in Figure 5 using kmeans clustering. The lower threshold of $\Psi = 1.9$, which is linked to about three cracks of 0.5 mm width, is the result of a second clustering step and iterations with the classification model.[27]

First, this classification model must be introduced. A classification model predicts a category given a set of inputs.[28,29] The relationship between the inputs and the predictions is set via a training process. For example, whether a brick is of fired-clay or calcium-silicate, could be determined based on the colour in a photograph. When the photograph is redder, the brick is likely of clay, while a more even distribution between colours (red, green, and blue) would suggest a brick of calcium-silicate. A simple model could employ a linear relationship and determine the ratios of RGB, trained on pre-classified (tagged) photographs, to later make predictions between the two brick categories. Simple models can be trained analytically, while more complex models require dedicated software. For this work, MATLAB and its built-in training routines were employed. There are many types of classification models with different types of trainable parameters. For a classification problem with a small number of discrete categories and a few predictors, a classification tree will produce good results.

Second, relevant predictors should be defined. From Figure 5, it should be clear that drift can be used to predict damage, with larger values of damage associated with larger values of drift in a positive correlation. Additionally, Figure 6 compares the relationship between wall type and damage. The ratio of Ψ divided by drift shows that walls of the D type exhibited larger values of Ψ at lower drift when compared to the other wall types. Since D is a CaSi shear wall, it is reasonable that A, the fired-clay shear walls, display the second highest ratio. The material of the masonry is included in the wall type. In Figure 6, dots outside the whiskers of the box plot refer to values further than 1.5 times the interquartile

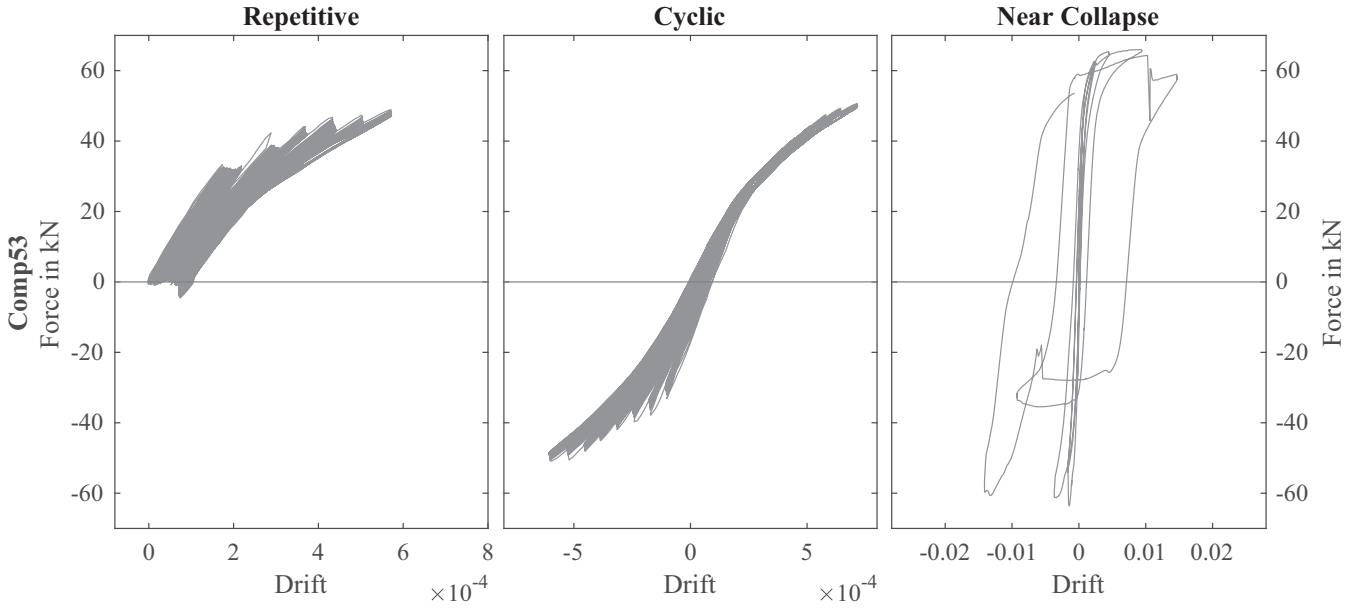

FIGURE 3 Example of the three experimental phases for wall Comp53 showing the force-drift curves. Note that the drift axes vary.

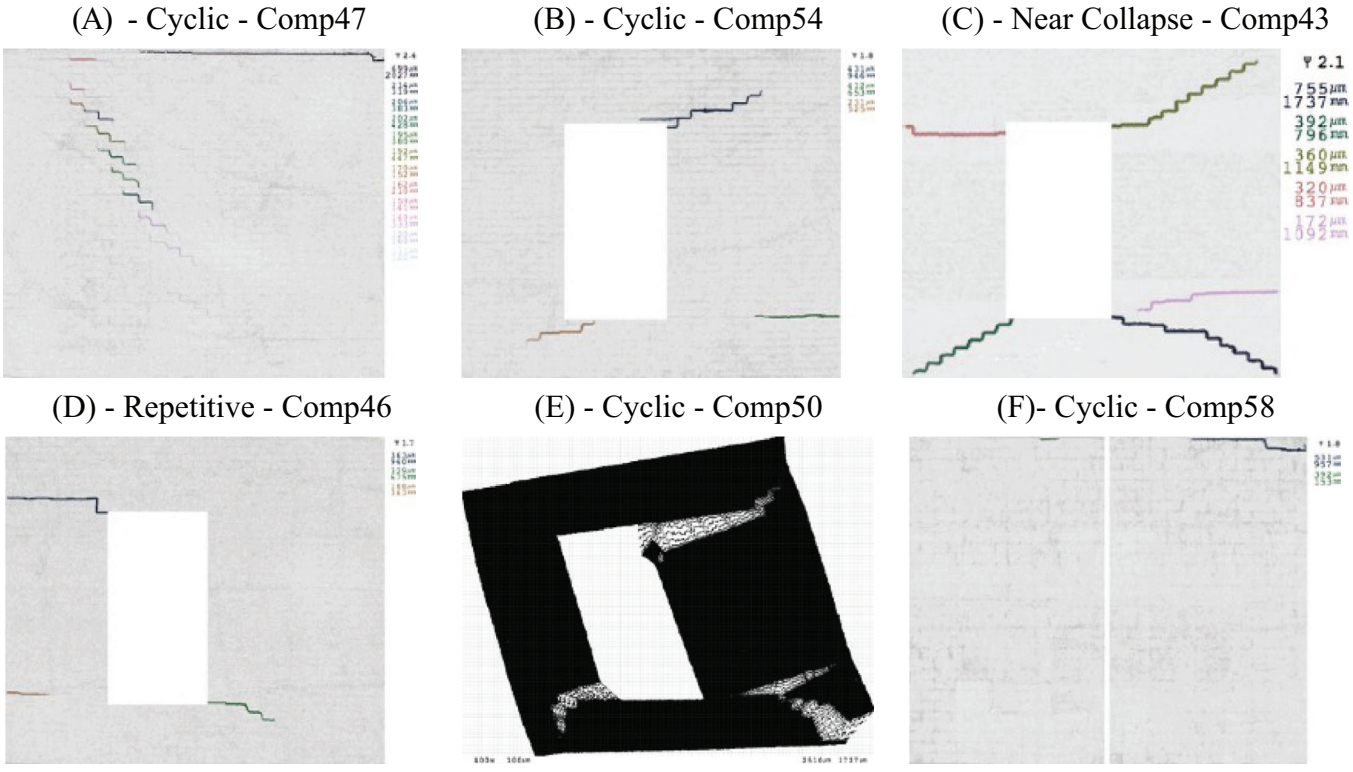

FIGURE 4 Examples of crack monitoring on various wall types during different protocol stages. For "E", a deformed shape, magnified 400×, is shown to depict the shape of the cracks.

range (IQR = Q3-Q1); since multiple specimens (especially for Types A and B) are tested and each comprises dozens of measurements, many 'outliers' are observed.

Two additional predictors are available: the boundary during the test that enforces a double-clamped or allows a cantilever condition, and the progress of the test. Since crack damage is accumulated throughout the test, towards the end, even at values of zero drift, residual cracks will be clearly visible. This means that identical values of drift will yield a

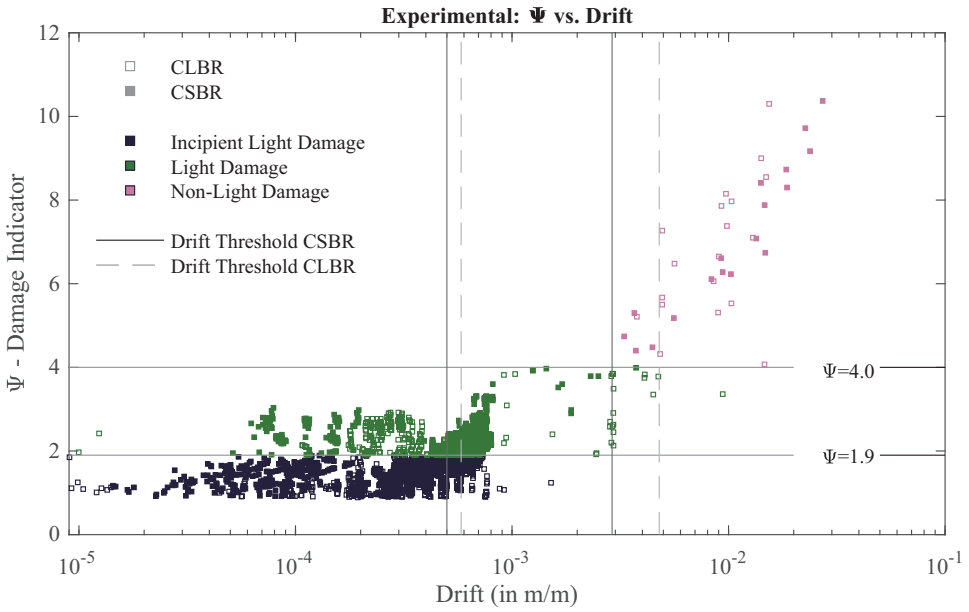

FIGURE 5 Wall in-plane drift against crack-based damage measured by Ψ. Proposed thresholds for fired-clay and calcium-silicate brick masonry are included; see next section.

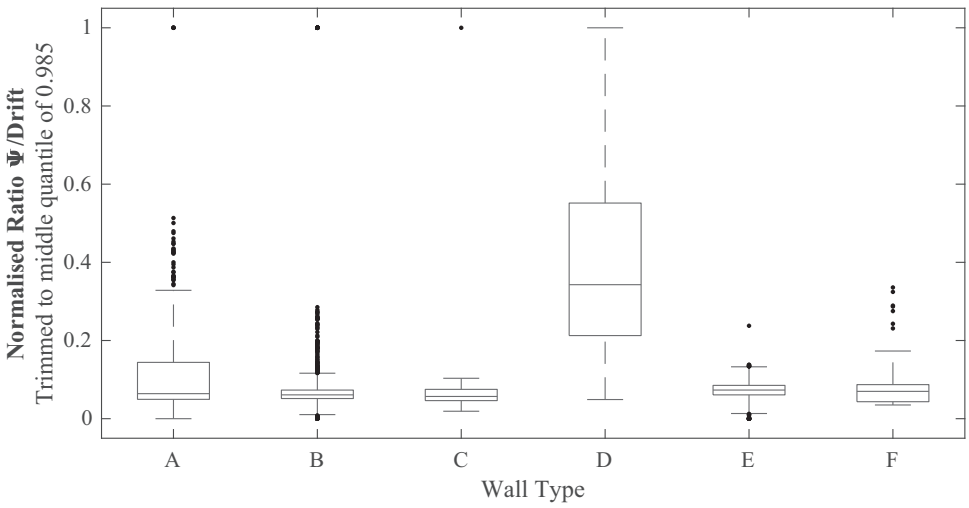

FIGURE 6 Influence of wall type, see Table 1. If Ψ and drift are linearly correlated, wall type D exhibits, on average, greater damage at equal drift compared to other wall types.

higher Ψ value if they occur later in the test. To investigate the influence of test progression, an indicator, linearly correlated between the first and last measurement instances, is introduced as additional feature. Furthermore, the data was pre-processed by taking the absolute values of drift and removing measurements with $\Psi = 0$, ultimately employing about six thousand data points.

3.2 | Classification decision tree

A decision tree creates nodes between branches to make decisions. For example, if the masonry is fired-clay, the tree would follow the left branch. Ultimately, every leaf at the end of each branch corresponds to a category. The number of times a certain predictor is used at the nodes to make a decision, corresponds to its importance. The aforementioned predictors are gathered in Table 2 where their importance is shown. Two variations are presented, one including the wall type as

TABLE 2 Description of various potential predictors for Ψ and their importance within a decision tree regression model. Wall type and masonry are mutually exclusive.

Predictor	Importance		Description
Drift	77.2%	79.5%	The in-plane wall drift measured during the tests
Test Progress	10.6%	11.9%	An indicator, linearly correlated between the first and last measurement instance
Wall Type	8.7%	NA	The geometry or type of wall, as per Table 1
Boundary	3.5%	3.4%	The test boundary, Cantilever or Fixed (double-clamped)
Masonry	NA	5.2%	The type of masonry, CLBR or CSBR, included in wall type

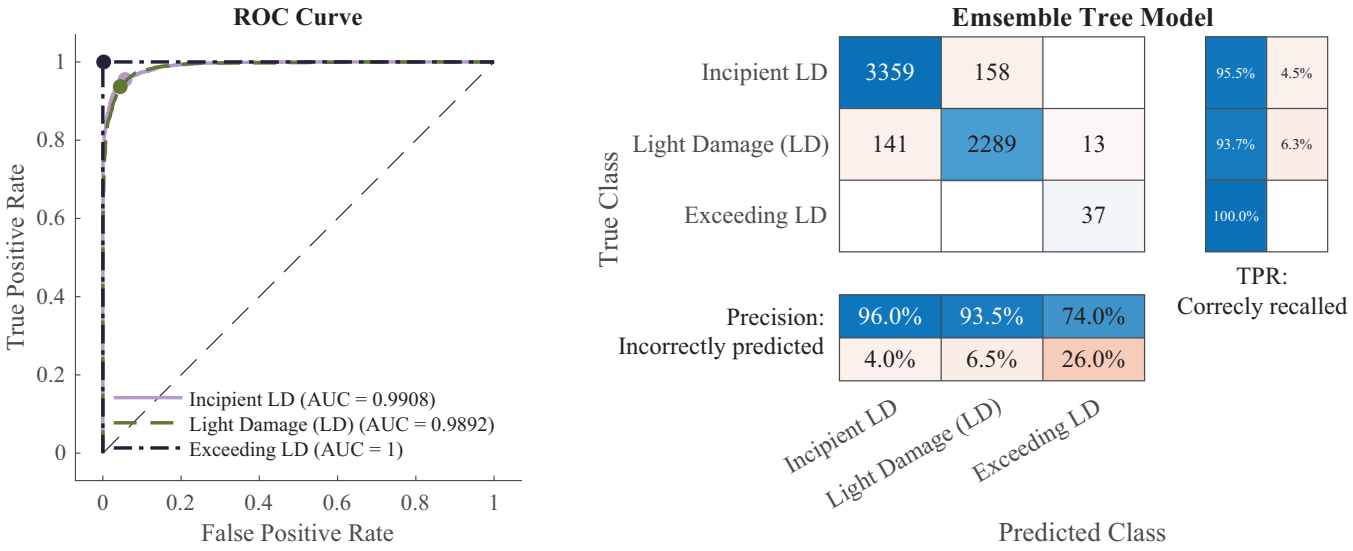

FIGURE 7 Confusion chart and ROC curve for an ensemble decision tree model with drift, wall type, boundary, and test progress as predictors of the damage class.

a predictor and another where only the masonry type is considered; these are mutually exclusive. The wall type, which contains more variability than the masonry type, is also a better predictor for damage, Ψ. The progression of the test is also associated with a relatively high importance of 10%. This means that damage does increase at repeated drift. However, larger values of drift are also imposed towards the end of the tests (as near collapse testing must follow the light damage protocol) so the relationship might be doubly correlated. Finally, the boundary of the test has the lowest importance. Whether the test was in cantilever or double-clamped form seems to be poorly related to the intensity of the cracks.

The performance of the classification model with the wall types can be evaluated using receiver operator curves (ROC) and confusion charts. These are displayed in Figure 7. An ROC plots the relationship between the true positive and false positive rate. Ideally, a model should never miss a true result, but this may come at the expense of outputting false positives. This balance can be tuned depending on the application and the desired type of outcome. For example, for this application, it is important that the model never misses a result that exceeds light damage (ELD). This is successfully achieved as evidenced by the 37 cases of ELD that are correctly identified by the model. However, the model also estimates 13 other cases (that were actually LD) as ELD; these are the false positives within the category of ELD. Between incipient LD and actual LD, the models are also capable of accurately recalling the true data values with more than 93% accuracy. This is verified by the high AUC (area under curve) values in the ROC plots. The threshold of $\Psi = 1.9$ for the beginning of LD, is determined by iteratively adjusting this value and observing the best accuracy and AUC rates.

3.3 | Simplified models for drift-Ψ

While the model with four predictors (drift, test progress, wall type and boundary) is very accurate, it requires several assumptions to be used in practice. For example, the type of wall will depend on the geometry and material of the wall

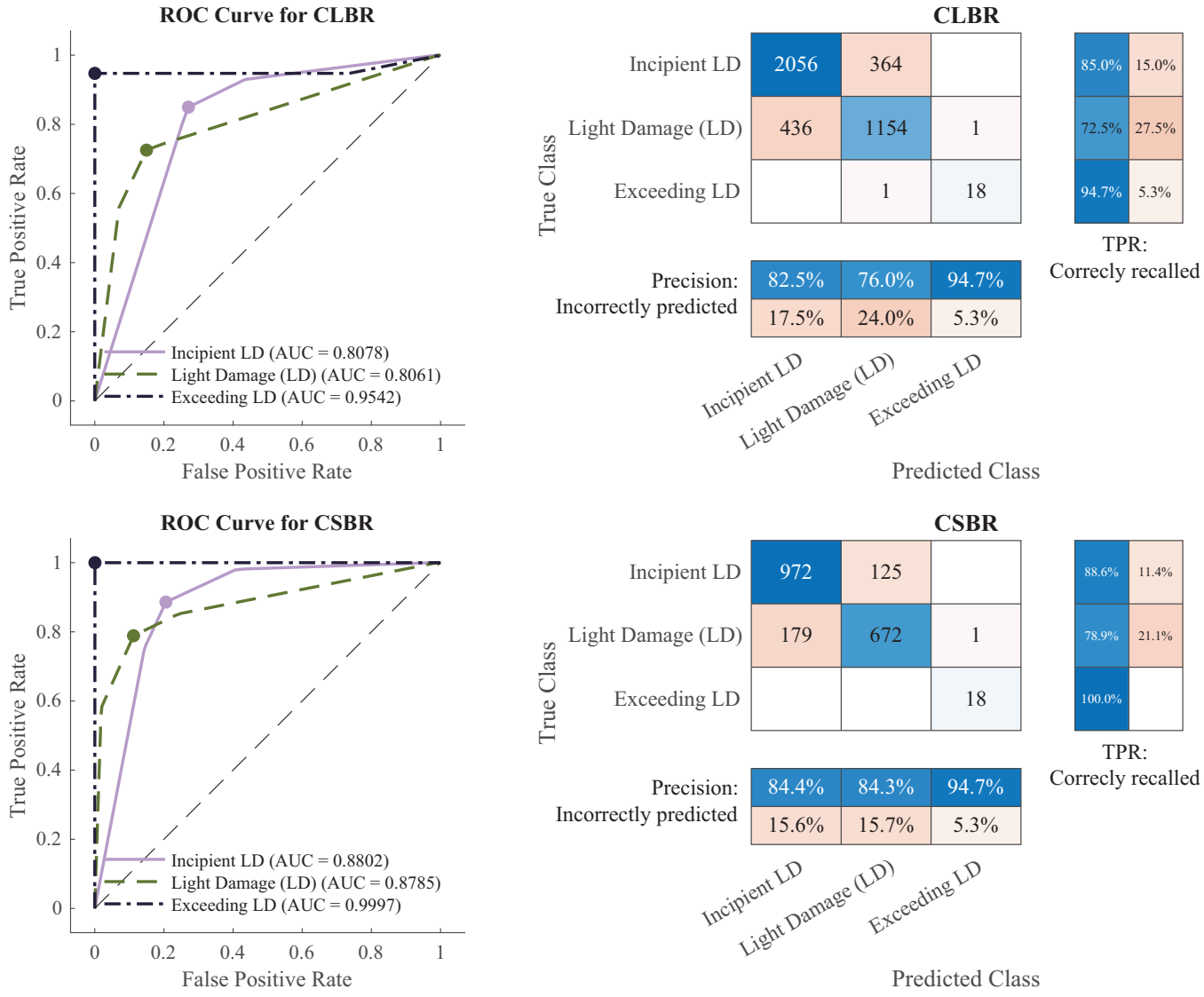

FIGURE 8 Confusion chart and ROC curve for clay brick masonry (top) and calcium–silicate brick masonry (bottom) using only drift and masonry as predictors of damage class.

being considered, the boundary will depend on its structural context, and the test progress will have to be linked, perhaps, to the age of the wall. The drift would be the design criteria to limit expected damage. Some of these assumptions can be difficult to define.

For this reason, a simpler model, considering only drift and masonry material as predictors, has been analysed. This can be more easily employed in practice and can be reduced to drift limits which do not require the trained model for making predictions. The performance of the model is segregated by masonry type, fired-clay (CLBR) or calcium–silicate (CSBR) brick masonry in Figure 8. The simpler model is less accurate than the full model; however, the high specificity for ELD is maintained with only 1 false positive for each model. Similarly, both ILD and LD are well discerned though some cross-predictions appear. In general, the models misclassify LD less often.

The results can be employed to derive the drift interval for which the models will classify a wall into light damage. These values are presented in Table 3. The beginning of LD is consistent between both types of material at about 0.05%, which is an incredibly small value of drift, about 1.35 mm for a wall of 2.7 m in height. The masonry will remain within LD for a reasonably long interval until a drift of 0.48 % for CLBR but only 0.29% for CSBR. Nevertheless, these values fall underneath drift limits employed to assess the ultimate capacity of masonry walls; see next section.

TABLE 3 Summary drift limits for each masonry type in mm/m or ‰.

Threshold	Fired-clay brick masonry	Calcium–silicate brick masonry
Start of light damage	0.58‰	0.50‰
End of light damage	4.8‰	2.90‰

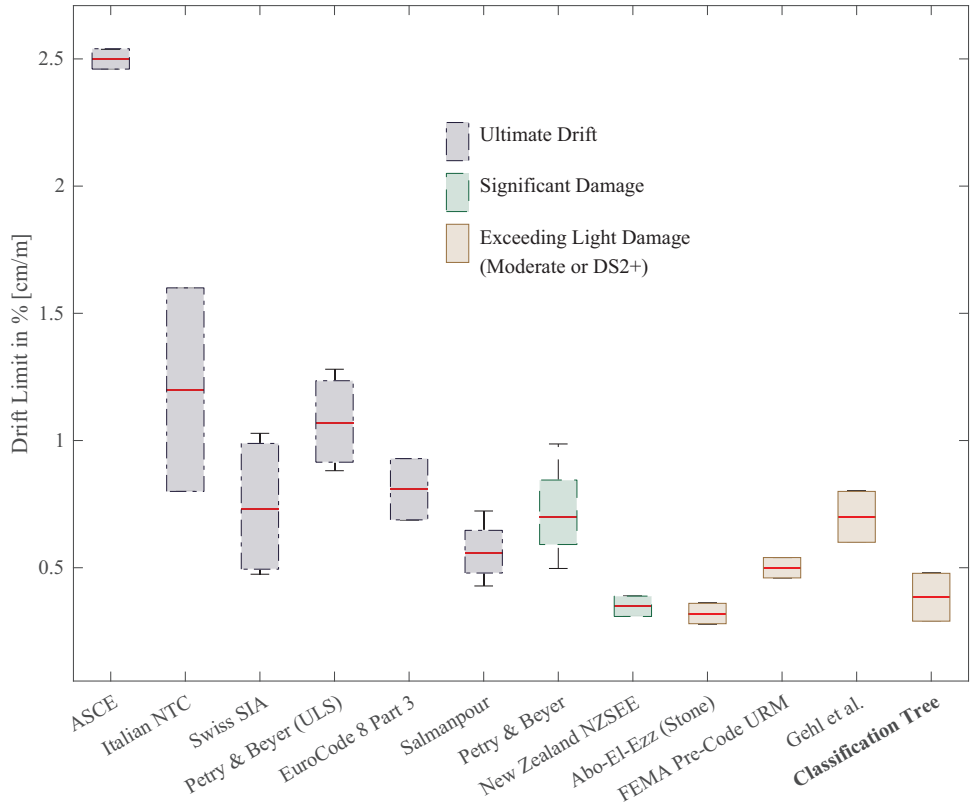

FIGURE 9 Comparison with other drift limits for various damage thresholds.

4 | DISCUSSION

Guidelines, codes and the work of many authors[1,3,17,30–35] have focused on establishing drift limits related to the ultimate capacity of masonry components. Some authors have derived limits associated with the lower damage states as extrapolations from ultimate drift values. Figure 9 provides an overview of comparisons against limits defined for ULS, for 'significant damage' (SD), and for DS2. Since different approaches consider different parameters, such as the overburden, the compressive strength of the masonry, the height of the walls or only the rotating height of a pier, the expected failure mechanism, etc., for the various walls tested, a range of limits are often obtained depending on the multiple assumptions; these are plotted in a box graph where the middle horizontal lines depict the mean values and the boxes indicate the interquartile range. For this comparison, the individual walls from this study are not observed, but the thresholds defined with the classification tree are used.

The first premise is that ULS limits should be higher than those for lower damage states. Indeed, all formulations result in values larger than the value determined for the upper threshold of light damage. The Italian guideline[31] for example, prescribes values for ultimate drift between 0.6% for shear walls and 1.8% for rocking masonry piers. Both values are significantly higher than that determined herein for the end of light damage at 0.5%. Employing the formulation from the ASCE,[33] results in even larger expected ultimate drift values of 2.5%.

The second premise is that limits for significant damage (SD) should be right at the end of the light damage range. Petry, Beyer[17] propose limits both for ULS and SD, the latter directly preceding the former and slightly above the values defined by the classification model. The New Zealand code[32] also prescribes values for SD which should correspond to the end of light damage. This seems to agree well with the values derived from the experiments. Similarly, FEMA[1] also specifies

drift values to be used for the analysis of pre-code unreinforced masonry structures; this describes the type of masonry components tested and matches well with the drift values obtained.

With a limited data set part of earlier work, Korswagen et al.[20] deduced that DS1 would occur for drift values between 0.3% and 1.1 ‰ for fired-clay brick walls in cantilever tests. Note that the damage state is a range of drift values and not a single threshold. As such, the starting threshold is slightly lower than observed herein with the extended data and a more rigorous analysis. The upper threshold, however, is significantly lower. This is because the earlier work investigated only DS1 and forwent DS2 even though the distinctions between the two are seldom strictly defined. In this paper, the first two states are clustered into the light damage category, distinguishing between light damage and exceeding it. The upper threshold of light damage in this paper does not necessarily correspond to significant damage or the ultimate limit state, nor is it strictly linked to DS3 or DS4. In Figure 5, the region above the threshold for ELD was simply denoted as non-light-damage; where additional threshold linked to the EMS damage scale for example, would be placed, has not been explored. In general, light damage could be considered to exclude structural repairs and require only aesthetic- and durability-focused repairs.

Furthermore, the difference in thresholds for masonry made from fired-clay or calcium-silicate units must be noted. While the mortar joints and unit sizes are similar, the material of the bricks differs. The drift at which light damage begins is comparable for both types; however, the drift at which light damage is exceeded is about 40% lower for calcium-silicate units. This makes calcium–silicate brick masonry more vulnerable to in-plane inter-storey drift, potentially due to its cracking behaviour, which involves brick-splitting and fewer but wider cracks. Nevertheless, it should be noted that CaSi brick masonry structures may, in fact, sustain less damage than their clay counterparts after earthquake loading because they experience reduced drift. This difference arises from the distinct structural contexts in which these materials are used. In the Netherlands, CaSi masonry structures are typically found in modern buildings with reinforced foundations, rigid floor diaphragms, and updated construction methods that better control inter-storey drift. Whether CaSi structures experience the same inter-storey drift as fired-clay brick structures when subjected to damaging actions such as vibrations or settlements, and whether they would consequently sustain more damage, still requires further investigation.

Finally, the drift limits obtained are linked to the thresholds set for the values of Ψ. A lower Ψ value marking the transition between incipient and light damage will also result in a lower drift value for this threshold. However, this also depends on the available experimental data which is most dense at lower Ψ values. For the upper threshold, clustering of the data was used to determine $\Psi = 4$; yet, this threshold is not very sensitive, with values between 3.7 and 4.0 leading to essentially identical upper drift limits (though different in terms of model accuracy). In terms of related cracks, with more than one crack at least 5 mm wide, this upper threshold is also reasonable and comparable to popular damage scales.[4,36] The threshold for the beginning of light damage is more sensitive. The strictest formulations consider a crack width of 0.1 mm ($\Psi = 1$), just visible, and some begin at 1 mm ($\Psi = 2$). Multiple cracks also affect the value of Ψ, so three cracks of 0.5 mm will already reach $\Psi = 1.9$. This seems like a reasonable compromise the consider a realistic start of light damage without falling into the most rigorous definition. Moreover, this value is associated with the best model prediction parameters.

The thresholds linked to Ψ are thus connected to the limitations of this damage parameter, too. Currently, the damage intensity depends only on the number of cracks, length and width, but does not consider whether the cracks appear in the mortar, at the mortar–brick interface, or through the bricks, the latter requiring more expensive repairs, and hence, linked to higher damage. Whether cracks are tapered, follow a uniform opening scheme or consist mostly of sliding, is also not considered, and this could be related to the causes of damage but also to specific repair measures. Some authors propose other formulations[37] to assess damage that could be used to consider these effects, especially if used in combination with computer-vision techniques,[38] yet these require more extensive post-processing and cannot always be employed. Nevertheless, the experimental data collected, including the high-resolution DIC measurements, could be re-assessed in the future using alternative definitions to explore different types of limits.

The findings presented in this study significantly advance our understanding of drift limits for masonry under light damage conditions, employing experimentally-derived data to establish robust thresholds. However, it is important to acknowledge the limitations inherent to the experimental setup. The study focused primarily on two types of masonry—fired-clay and calcium-silicate brick masonry. While these materials are commonly used, the generalisability of the results to other masonry types, such as those involving different brick compositions or mortar types, remains to be tested. Future research could expand on this work by incorporating a broader variety of masonry materials, which would help in validating and possibly refining the drift limits proposed here.

Moreover, while the study provides a comprehensive analysis of crack-based damage as a function of in-plane drift, the application of the findings to real-world scenarios requires careful consideration. The experimental conditions, although

meticulously controlled to replicate actual loading conditions as closely as possible, still represent a simplification of the complex interactions and variables present in actual structures. For instance, the impact of mixed in-plane and out-of-plane loading, was not within the scope of this investigation. Integrating these factors into future experimental designs could significantly enhance the practical applicability of the drift limits defined. Additionally, further studies could explore the effect of repeated load cycles over extended periods to better simulate the aging and creep processes of masonry structures.

4.1 | Limitations

This study presents a detailed examination of drift limits for masonry components under various damage conditions, yet it is accompanied by several limitations. First, the generalisability of the findings is constrained by the focus on only two types of masonry—fired-clay and calcium-silicate brick masonry. The application of these results to other masonry types involving different brick compositions or mortar types remains untested, suggesting a potential avenue for future research to broaden the validation of these drift limits. Additionally, while the experimental setup was carefully controlled to mimic real loading conditions, it inherently simplifies the complex interactions and variables present in actual structures, such as mixed in-plane and out-of-plane loading or restrained lateral edges, which were not considered in this study. Similarly, while some walls experienced toe-crushing, higher overburdens might lead to more widespread compressive failure. These limitations underscore the need for integrating these factors in future experimental designs to enhance the practical applicability of the established drift limits. Moreover, the study does not account for the effects of repeated load cycles over extended periods, which could better simulate the aging and creep processes in masonry structures. Lastly, the thresholds linked to the Ψ values also bear limitations, as the current damage intensity assessment relies solely on the number and dimensions of cracks without considering their locations or the nature of crack openings, which could significantly influence repair strategies and costs. Future studies could benefit from re-assessing the experimental data with alternative definitions or employing computer-vision techniques to explore different types of limits and more accurately assess damage.

5 | CONCLUSIONS

Results from experimental campaigns on masonry walls have been reinterpreted by post-processing digital image correlation measurements into a crack-based metric and relating it to the in-plane drift of the walls at every measurement instance. Then, the relationship between drift and damage has been explored using a classification model where other predictors are considered. Besides drift, which was found to be highly correlated to damage, the wall type and its material, the boundary of the experimental setup, and the progress of the test were found to be linked to damage. The latter considered that repeated values of drift, occurring later in the tests, were linked to slightly higher damage. Similarly, walls with a cantilever boundary could sustain a slightly larger drift before displaying the same intensity of crack damage than walls subjected to a double-clamped boundary. Moreover, shear walls displayed larger cracks than walls with an opening at similar drift. Analogously, calcium-silicate (CaSi) walls showed more intense damage than fired-clay brick walls. In fact, when simplifying the classification model to consider only the drift and the masonry material as predictors to establish drift limits for the interval of light damage, CaSi masonry obtained an upper limit 40% lower than fired-clay brick masonry, which exceeds light damage at a value of 0.5%. The upper crack-based light damage threshold corresponds to about three cracks of 6 mm in width. The beginning of light damage, with visible cracks about 1 mm wide, occurs at 0.5 and 0.6‰ for CaSi and clay, respectively.

These thresholds may be used directly when designing for performance goals that limit 'significant damage' or even address the serviceability limit state. Older structures, or masonry that is expected to be subjected to a large number of load repetitions, should be evaluated with slightly reduced drift values (about 10%). Likewise, shear walls, or squat walls connected to rigid floors and foundations, should also consider limits reduced by a similar amount.

Finally, it must be highlighted that these experimentally-derived limits are still related to decisions about the crack-based boundaries for light damage, with inevitably remain somewhat arbitrary. Moreover, future tests should consider additional repetitions to obtain richer drift data around the upper threshold of light damage, which is now slightly scarce.

ACKNOWLEDGEMENTS

The authors would like to acknowledge funding by NAM (Nederlandse Aardolie Maatschappij) and IMG (Instituut Mijnbouwschade Groningen) which was used to conduct the experiments. The invaluable contribution of Dr. Edwin Meulman and Belen Gaggero (MSc) for the successful realisation of these experiments is also highlighted along with the support of laboratory staff at the TU Delft. Finally, thanks go to Michele Longo (MSc) for shaping the overall campaign with pre- and post-diction numerical models.

DATA AVAILABILITY STATEMENT

The experimental data that support the findings of this study are openly available in 'Data underlying the PhD thesis: Quantifying the probability of light damage to masonry structures—An exploration of crack initiation and progression due to seismic vibrations on masonry buildings with existing damage' at 4TU.ResearchData via https://doi.org/10.4121/58d1f5e6-5db3-4a74-a3d1-6e88a3bd8bce.

ORCID


Paul A. Korswagen https://orcid.org/0000-0002-2587-7808

REFERENCES

1. FEMA. Hazus MH MR5. FEMA. 2013
2. Crowley H, Pinho R, Polidoro B, van Elk J. Developing fragility and consequence models for buildings in the Groningen field. *Netherl J Geosci.*;96:s247-s257. 96-95 2017s247–s257.
3. Messali F, Rots JG. In-plane drift capacity at near collapse of rocking unreinforced calcium silicate and clay masonry piers. *Eng Struct*. 2018;164(2018):183-194.
4. Burland JB, Wroth CP, Settlement of buildings and associated damage. Proceedings of Conference on Settlement of Structures, pages 611-654, Cambridge, 1974. Pentech Press.
5. Del Gaudio C, De Risi MT, Ricci P, Verderame GM. *Drift-based fragility functions for hollow clay masonry infills in RC buildings under in-plane seismic actions*. 2017. Anidis.
6. Van Staalduinen PC, Terwel K, Rots JG. *Onderzoek naar de oorzaken van bouwkundige schade in Groningen Methodologie en case studies ter duiding van de oorzaken*. Delft University of Technology; 2018. www.NationaalCoordinatorGroningen.nl. Report number CM-2018-01.
7. Aldemir A, Binici B, Canbay E, Yakut A. Lateral load testing of an existing two-story masonry building up to near collapse. *Bull Earthquake Eng*. 2015. doi:10.1007/s10518-015-9821-3
8. Esposito R, Messali F, Ravenshorst GJP, Schipper HR, Rots JG. Seismic assessment of a lab-tested two-storey unreinforced masonry Dutch terraced house. *Bull Earthquake Eng*. 2019;17:4601-4623. doi:10.1007/s10518-019-00572-w
9. Grottoli L, Kallioras S, Korswagen P, Graziotti F. In-plane and out-of-plane quasi-static cyclic tests on unreinforced calcium-silicate masonry walls under high compressive load. *EUCENTRE Foundation*. 2019. www.eucentre.it/nam-project. Technical Report EUC067/2019U. Pavia, Italy. Available online at.
10. Colangelo F. On the code-compliant verification of seismic damage to non-structural masonry infills. *Bull Earthquake Eng*. 2015;13:2051-2072. doi:10.1007/s10518-014-9704-z
11. Grünthal G, Musson RMW, Schwarz J, Stucchi M. European macroseismic scale 1998 (EMS-98). *Eur Seismol Commission, sub commission on Engineering Seismology*. 1998;15. Working Group Macroseismic Scales. Conseil de l'Europe, Cahiers du Centre Européen de Géodynamique et de Séismologie.
12. Crowley H, Pinho R, Cavalieri F, Report on the v6 Fragility and Consequence Models for the Groningen Field. NAM. 2019
13. Gehl P, Seyedi DM, Douglas J. Vector-valued fragility functions for seismic risk evaluation. *Bull Earthquake Eng*. 2013;11:365-384. doi:10.1007/s10518-012-9402-7
14. Magenes G, Calvi GM. In-plane seismic response of brick masonry walls. *Earthq Eng Struct Dyn*. 1997;26:1091.
15. Magenes G, Penna A, Galasco A, Paré MD, In-plane cyclic shear tests of undressed double-leaf stone masonry panels. 8th International Masonry Conference 2010 in Dresden. 2010.
16. Graziotti F, Rossi A, Mandirola M, Penna A, Magenes G, Experimental characterisation of calcium-silicate brick masonry for seismic assessment. 16th International Brick and Block Masonry conference ISBN 978-1-138-02999-6. 2016.
17. Beyer K, Mergos P, Sensitivity of drift capacities of urm walls to cumulative damage demands and implications on loading protocols for quasi-static cyclic tests. 12th North American Masonry Conference, Denver, Colorado. May 17–20, 2015.
18. Negulescu C, Ulrich T, Baills A, Seyedi DM. Fragility curves for masonry structures submitted to permanent ground displacements and earthquakes. *Nat Hazards*. 2014;74:1461-1474. doi:10.1007/s11069-014-1253-x
19. Petry S, Beyer K. Limit states of modern unreinforced clay brick masonry walls subjected to in-plane loading. *Bull Earthq Eng*. 2015;13:1073-1095. doi:10.1007/s10518-014-9695-9
20. Korswagen PA, Longo M, Meulman E, Rots JG. Crack initiation and propagation in unreinforced masonry specimens subjected to repeated in-plane loading during light damage. *Bull Earthq Eng*. 2019. doi:10.1007/s10518-018-00553-5

21. Korswagen PA, Longo M, Rots JG. High-resolution monitoring of the initial development of cracks in experimental masonry shear walls and their reproduction in finite element models. *Eng Struct*. 2020;211:110365.
22. Korswagen PA, Longo M, Rots JG. Calcium silicate against clay brick masonry: an experimental comparison of the in-plane behaviour during light damage. *Bull Earthq Eng*. 2020;18:2759-2781. doi:10.1007/s10518-020-00803-5
23. Korswagen PA, Rots JG, Monitoring and quantifying crack-based light damage in masonry walls with digital image correlation. Proceedings of 1st International Conference on Structural Damage Modelling and Assessment, Lecture Notes in Civil Engineering. 110. 2020. doi:10.1007/978-981-15-9121-1_1
24. Ghorbani R, Matta F, Sutton MA. Full-field deformation measurement and crack mapping on confined masonry walls using digital image correlation. *Exp Mech*. 2015;55:227-243.
25. Likas A, Vlassis N, Verbeek JJ. The global k-means clustering algorithm. *Pattern Recogn*. 2003;36:451-461. doi:10.1016/S0031-3203(02)00060-2
26. Narassiguin A, Bibimoune M, Elghazel H, Aussem A. An extensive empirical comparison of ensemble learning methods for binary classification. *Pattern Anal Applic*. 2016;19:1093-1128. doi:10.1007/s10044-016-0553-z
27. Oses N, Dornaika F, Moujahid A. Image-based delineation and classification of built heritage masonry. *Remote Sens*. 2014;6:1863-1889. doi:10.3390/rs6031863
28. Sharafati A, Asadollah SBHS, Al-Ansari N. Application of bagging ensemble model for predicting compressive strength of hollow concrete masonry prism. *Ain Shams Eng J*. 2021;12:3521-3530. doi:10.1016/j.asej.2021.03.028
29. Son H, Kim C, Hwang N, Kim C, Kang Y. Classification of major construction materials in construction environments using ensemble classifiers. *Adv Eng Inf*. 2014;28:1-10. doi:10.1016/j.aei.2013.10.001
30. SIA, SIA 266. Mauerwerk. *Swiss Society of Engineers and Architects (SIA)*, 2015 [in German].
31. MIT MI and Transportations. NTC. Decreto Ministeriale 14/1/2008: Norme tecniche per le costruzioni, G.U.S.O. n.30 on 4/2/2008 [in Italian]. 2008
32. NZSEE, New Zealand Society for Earthquake Engineering. *The seismic assessment of existing buildings, Part C8: Seismic assessment of unreinforced masonry buildings*. MBIE, EQC, SESOC, NZSEE and NZGS, 2017.
33. ASCE, American Society of Civil Engineers. *Seismic Evaluation and Retrofit of Existing Buildings (ASCE/SEI 41-13)*. 2014.
34. CEN E. *Committee for Standardisation. Eurocode 8: Design of structures for earthquake resistance—Part 3: general rules, seismic actions and rules for buildings*. 2005. EN 1998-3.
35. Salmanpour AH, Schwartz NMJ. Displacement capacity of contemporary unreinforced masonry walls: an experimental study. *Eng Struct*. 2015;89:1-16.
36. Giardina G, van de Graaf AV, Hendriks MAN, Rots JG, Marini A. Numerical analysis of a masonry façade subject to tunnelling-induced settlements. *Eng Struct*. 2013;54:234-247.
37. Sarhosis V, Dais D, Smyrou E, Bal IE, Drougkas A. Quantification of damage evolution in masonry walls subjected to induced seismicity. *Eng Struct*. 2021;243:112529. doi:10.1016/j.engstruct.2021.112529
38. Dais D, Bal IE, Smyrou E, Sarhosis V. Automatic crack classification and segmentation on masonry surfaces using convolutional neural networks and transfer learning. *Autom Constr*. 2021;125:103606. doi:10.1016/j.autcon.2021.103606

How to cite this article: Korswagen PA, Rots JG, Terwel KC. Experimentally-based in-plane drift limits for the upper threshold of masonry light damage. *Earthquake Engng Struct Dyn*. 2024;1-14. https://doi.org/10.1002/eqe.4246